

See discussions, stats, and author profiles for this publication at: <https://www.researchgate.net/publication/221769580>

Effects of Charge Location on the Absorptions and Lifetimes of Protonated Tyrosine Peptides in Vacuo

ARTICLE *in* THE JOURNAL OF PHYSICAL CHEMISTRY A · FEBRUARY 2012

Impact Factor: 2.69 · DOI: 10.1021/jp208578w · Source: PubMed

CITATIONS

4

READS

22

6 AUTHORS, INCLUDING:



Jb Greenwood

Queen's University Belfast

99 PUBLICATIONS 764 CITATIONS

[SEE PROFILE](#)



Steen Brøndsted Nielsen

Aarhus University

197 PUBLICATIONS 3,072 CITATIONS

[SEE PROFILE](#)

Effects of Charge Location on the Absorptions and Lifetimes of Protonated Tyrosine Peptides in Vacuo

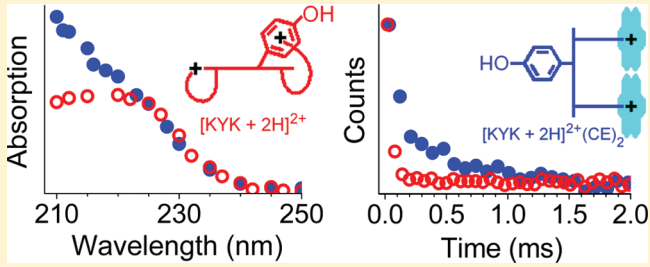
Orla Kelly,[†] Christopher R. Calvert,[†] Jason B. Greenwood,[†] Henning Zettergren,[‡]
Steen Brøndsted Nielsen,[§] and Jean A. Wyer*,[§]

[†]Centre for Plasma Physics, School of Mathematics and Physics, Queen's University Belfast, BT7 1NN, U.K.

[‡]Department of Physics, Stockholm University, SE-10691 Stockholm, Sweden

[§]Department of Physics and Astronomy, Aarhus University, Ny Munkegade, DK-8000 Aarhus C, Denmark

ABSTRACT: Nearby charges affect the electronic energy levels of chromophores, with the extent of the effect being determined by the magnitude of the charge and degree of charge-chromophore separation. The molecular configuration dictates the charge–chromophore distance. Hence, in this study, we aim to assess how the location of the charge influences the absorption of a set of model protonated and diprotonated peptide ions, and whether spectral differences are large enough to be identified. The studied ions were the dipeptide YK, the tripeptide KYK (Y = tyrosine; K = lysine) and their complexes with 18-crown-6-ether (CE). The CE targets the ammonium group by forming internal ionic hydrogen bonds and limits the folding of the peptide. In the tripeptide, the distance between the chromophore and the backbone ammonium is enlarged relative to that in the dipeptide. Experiments were performed in an electrostatic ion storage ring using a tunable laser system, and action spectra based on lifetime measurements were obtained in the range from 210 to 310 nm. The spectra are all quite similar though there seems to be some changes in the absorption band between 210 and 250 nm, while in the lower energy band all ions had a maximum absorption at ~275 nm. Lifetimes after photoexcitation were found to shorten upon protonation and lengthen upon CE complexation, in accordance with the increased number of degrees of freedom and an increase in activation energies for dissociation as the mobile proton model is no longer operative.



1. INTRODUCTION

Absorption by proteins in the near UV region is due to the absorption of their constituent aromatic amino acids phenylalanine (Phe, F), tryptophan (Trp, W), and tyrosine (Tyr, Y). The exact position of the absorption bands, however, depends on the microenvironment of the chromophores, with shifts due to solvation, the proximity of charges and nearby amino acid residues. Thus, while in certain cases, the best way to approximate the environment of a buried chromophore is to assume it is in a vacuum, (e.g., the green fluorescent protein),¹ in other cases, the amino acid residues in the neighborhood of the chromophore are known to play a significant role (e.g., absorption by protonated Schiff-base retinal, the chromophore responsible for vision).^{2,3} This sensitivity of the photophysics (i.e., absorption, fluorescence, and vibrational signatures) of phenylalanine, tyrosine, and tryptophan to their chemical environment makes these amino acids highly important spectroscopic probes for protein conformations and dynamics.^{4,5} Exploitation of the chromophores' photophysics as spectroscopic probes relies on in-depth knowledge of precisely how the photophysics changes with the microenvironment. This provides the motivation for our present work in which the effect of a nearby charge on the absorption bands of the tyrosine chromophore is studied.

Developments in mass spectrometry have allowed for studies of fragile ions isolated in the gas phase, and in recent years, a significant amount of spectroscopy work has been conducted for protonated amino acids and small protonated peptides.^{6–22} In our Aarhus laboratory, gas-phase absorption spectroscopy on macromolecular ions has been made possible from the combination of an electrospray ion source, an electrostatic ion storage ring, and pulsed lasers.^{23,24} In the ring, ions are photoexcited, and their lifetimes, with respect to dissociation, are measured. The problem with finite sampling intervals encountered when using finite length time-of-flight instruments (kinetic shifts) is often circumvented, and the actual number of photoexcited ions at all wavelengths may be obtained from fits to exponential decays of the ions. Our method differs from the conventional approach, where absorption spectra are measured by quantifying the loss of light after irradiation of a sample. Such light transmission experiments are employed for measurements of neutral molecules in the gas phase, while for ions, it is difficult to produce a vast enough number of ions. The method used here to identify photon absorption relies on the detection of fragmentation and is called action spectroscopy.

Received: September 6, 2011

Revised: January 20, 2012

Published: January 23, 2012

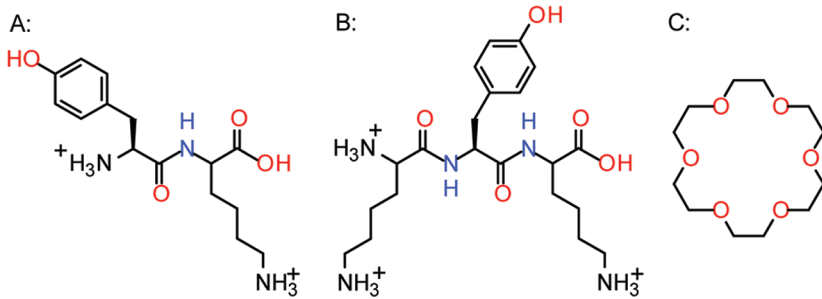


Figure 1. Structures of (A) $[YK + 2H]^{2+}$, (B) $[KYK + 3H]^{3+}$, and (C) 18-crown-6-ether (CE). The likely protonation sites are indicated.

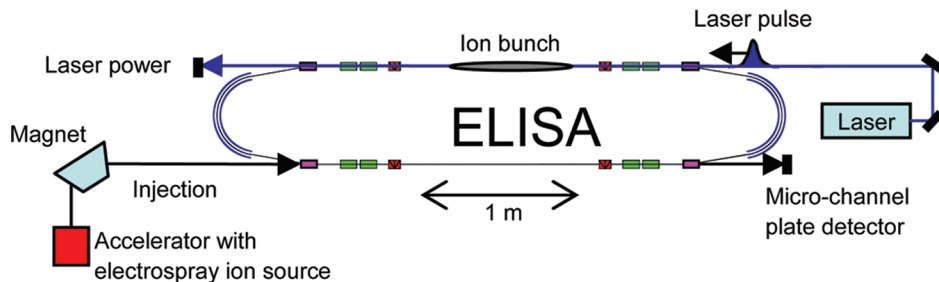


Figure 2. Schematic of the ELISA electrostatic storage ring in combination with a laser system. The photofragment yield was obtained as a function of wavelength from the signal of neutrals hitting the detector.

Previous studies have shown that protonated tyrosine has absorption band maxima at 225 nm²¹ and 275 nm.²⁵ In molecules containing tyrosine, the positions of these bands are dependent on the local environment. For example, perturbations in these band maxima were seen for protonated dipeptides containing alanine and tyrosine and their complexes with 18-crown-6-ether (CE), with relative shifts up to 6 and 5 nm for the high- and low-energy bands, respectively.²¹ Water was found to cause a redshift of the lower energy band by ~5 nm, typical for $\pi\pi^*$ transitions. This is in contrast to work by Bellina et al.,²⁶ where it was found that for the tyrosine-containing protein ubiquitin (charge state -6), where the tyrosines are particularly sensitive to the outside environment, the absorption by the $\pi\pi^*$ band is red-shifted after desolvation. This red-shift may be due to the presence of a negative charge in the vicinity of the tyrosine in the gas phase, and the authors hence conclude that the shift between the solution and the gas phase could be due to the addition of several contributions with opposite effects. Another tyrosine-containing protein is insulin. Antoine et al.²⁵ studied the $[insulin-4H]^4$ ion, where the four tyrosines are neutral and found that the absorption band was red-shifted to a maximum at 281 nm and was broader than the absorption band for bare protonated tyrosine. For the $[insulin-6H]^{-6}$ ion, a band at 264 nm was seen, along with absorption above 300 nm, which is due to the deprotonation of one of the four tyrosine phenol groups.¹⁸

In order to further elucidate the effect of a nearby charge on the absorption bands of tyrosine, we have in this work studied a group of model systems, namely, the peptides YK and KYK (Figure 1). Conformational search calculations by Prell et al.²⁷ found at least 1000 structures within 50 kJ/mol of the lowest-energy structure for the $[KYK + 2H]^{2+}$ ion, suggesting that numerous folding motifs are present at room temperature. Furthermore, the authors found that in the majority of low-energy structures, the protonated amines each form one or more hydrogen bonds to polarizable atoms in the peptide. Hence, in our work, modification of the charge–chromophore

interaction was achieved in several ways, either by varying the distance between the backbone ammonium and the chromophore (dipeptide vs. tripeptide), by changing the charge state of the peptides or by altering folding motifs through the use of CE. The size of the chosen crown ether is optimum for the formation of three hydrogen bonds with ammonium,^{28–30} and it prevents the occurrence of the dominant folding motifs, which are as a result of ionic charges interacting with polar groups. At the same time, the large size of the crown ether sterically reduces folding. The side chain is, therefore, prevented from interacting with either the ammonium group or the phenol ring. We do not know the actual structures of these complexes, but there is no doubt that they are different to those of the uncomplexed dipeptides and tripeptides.

2. EXPERIMENTAL SECTION

Experiments were carried out at the electrostatic ion storage ring in Aarhus (ELISA) (see Figure 2).²³ All compounds were purchased from Sigma-Aldrich. The charges were carried either on the N-terminal amino group or on a side chain (Figure 1). Electrospray ionization was used to produce the ions that were subsequently accumulated in a 22-pole ion trap and thermally equilibrated by collisions with a helium buffer gas therein. The ions were accelerated as an ion bunch to kinetic energies of 22 keV per charge, and a bending magnet was used to select the appropriate ions according to their mass-to-charge ratio. Following injection into the ring, the ions were stored for about 35 ms before being irradiated by a nanosecond light pulse from a tunable EKSPLA laser over the wavelength range 210–310 nm. This is an Nd:YAG laser where the third harmonic (355 nm) pumps an optical parametric oscillator (OPO). The visible output from this OPO is frequency doubled in a crystal providing UV light. The repetition rate of the experiment was 10 Hz. Lifetimes with respect to dissociation were obtained from measurements of the yield of neutrals hitting the microchannel plate (MCP) detector located at the end of the straight section opposite to the side where photoexcitation was

performed (i.e., delayed dissociation). It should be mentioned that because daughter ions have lower kinetic energies than those of the parent ions, they are not stored in the ring. An exception to this is dehydrogenated ions formed after a photoinduced loss of hydrogen since their kinetic energies are too close to those of the parent ions to be differentiated.³¹

The pressure in the ring was close to 10^{-10} mbar, which set an upper limit of seconds on the storage time.

3. RESULTS AND DISCUSSION

3.1. Calculations. In order to try to understand how the proximity of a charge to the chromophore may affect absorption, time-dependent density functional theory calculations³² were executed. The calculations were carried out on a typical low energy structure of the $[\text{KYK} + 2\text{H}]^{2+}$ ion as found by Prell and co-workers²⁷ by means of conformational searches using the MMFFs force fields. In our calculations, the structure was optimized at the B3LYP/3-21G level followed by frequency calculations to validate that it corresponds to a minimum on the potential energy surface. The excited state energies for this structure were then calculated by means of time-dependent density functional theory at the TDB3LYP/6-31+g(d,p) level using the Gaussian package.³² This showed that the excitations are not dominated by single electron–hole pairs from the set of ground state orbitals. Thus, in order to investigate the excited state characters, we performed a natural-transition-orbital (NTO) analysis³³ implemented in Gaussian. After the orbital transformation, the excitations were due to single electron–hole pairs that reproduced >80% of the transition density. Our calculated absorption spectrum is shown in Figure 3, while the NTO orbitals for the electron–hole pair of five prominent spectral lines (labeled I–V) in the 210–310 nm region are shown in Figure 4a. The NTO analysis shows that the lowest excitation energy at 284 nm (I) corresponds to a transition from the phenol ring to the peptide backbone. The same is true for the second lowest excitation energy at 261 nm (II), but the transition also contains some $\pi\pi^*$ character, while the transition with the third lowest excitation energy at 256 nm (III) instead has a more pure $\pi\pi^*$ character. It should be noted that TDDFT in general provides a rather poor description of charge transfer transitions with a typical error of a few tenths of an electronvolt, which may affect the ordering of the lowest excited states but not the overall trends. The lines carrying the strongest oscillator strengths at 227 nm (IV) and 221 nm (V) have rather different characters. While the former corresponds to a transition within the peptide backbone, the latter has a multiple character and is due to a transition from within the phenol ring, to the NH_3^+ group interacting with the ring, and to the peptide backbone. Thus, according to the calculations, one would expect rather weak absorption in the 250–280 nm region with a rapid increase in intensity in the 210–230 nm region, as suggested by the solid curve in which the peak half width is set to 0.3 eV mimicking typical experimental conditions.

The calculated results indicate that a nearby charge is likely to affect the absorption based on the direction of the transition dipoles relative to the positively charged ammonium group. In a previous work on singly and doubly protonated Oligo(p-phenyleneethynylene)s (OPEs),³⁴ we established a clear redshift of the absorption band upon single protonation and that a charge placed symmetrically on the other side of the conjugated network counteracted this effect. In the peptides studied in the present work, we vary the distance and

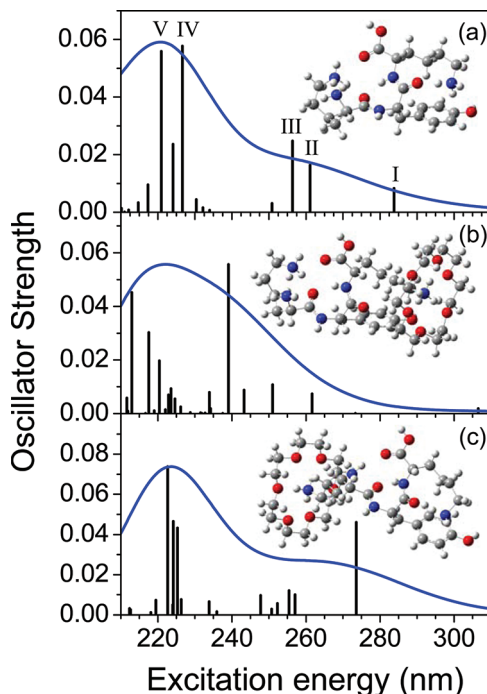


Figure 3. Oscillator strengths based on TDDFT (TDB3LYP/6-31+G(d,p)) calculations of (a) $[\text{KYK} + 2\text{H}]^{2+}$, (b) $[\text{KYK} + 2\text{H}](\text{CE})^{2+}$, where the CE is attached to the NH_3^+ group, which is interacting with the ring in the bare ion, and (c) $[\text{KYK} + 2\text{H}](\text{CE})^{2+}$, where the crown ether is attached to the NH_3^+ group on the other side chain. The blue lines were calculated under the assumption that the widths of the bands were 0.3 eV, which was the average value for the widths in a previous study. Optimized structures of the ions are also shown.

orientation between the phenol and the charge site by changing the peptide conformation through crown ether addition and looking at single versus double protonation.

To investigate how the charges affect the absorption behaviors, a crown ether was attached to either of the NH_3^+ groups. These structures were then relaxed by means of geometry optimizations at the B3LYP/3-21G level followed by excited state energy calculations at the TDB3LYP/6-31+g(d,p) level. The results are shown in Figure 3b,c and clearly show that crown ether addition changes the spectra. Unsurprisingly, it matters which ammonium group is targeted by the crown ether. In summary, the presence of a charge is predicted to affect the absorption, and the extent of this affect was next probed experimentally (see sections 3.2 and 3.3). It should be emphasized that in addition to those studied here, there are many other likely structures of the complexes.

Finally, we note that results for $[\text{KYK} + 2\text{H}]^{2+}$ calculated using the PBE0 functional or a larger basis set (6311+G(2d,p)) gave similar results to those obtained using the TDB3LYP/6-31+G(d,p) level of theory.

3.2. Lifetimes with Respect to Dissociation after Photoexcitation. Sample time spectra for each of the ions after 215 nm photoexcitation, measured by detecting the neutral fragments on one side of the ring, are shown in Figure 5. Because of the experimental setup, measured fragments were produced approximately half a revolution after photoexcitation in the first instance and then after successive rotations in the ring (see Table 1 for revolution times). It can be seen that for all the ions, dissociation is complete within 0.5 ms. Figure 6

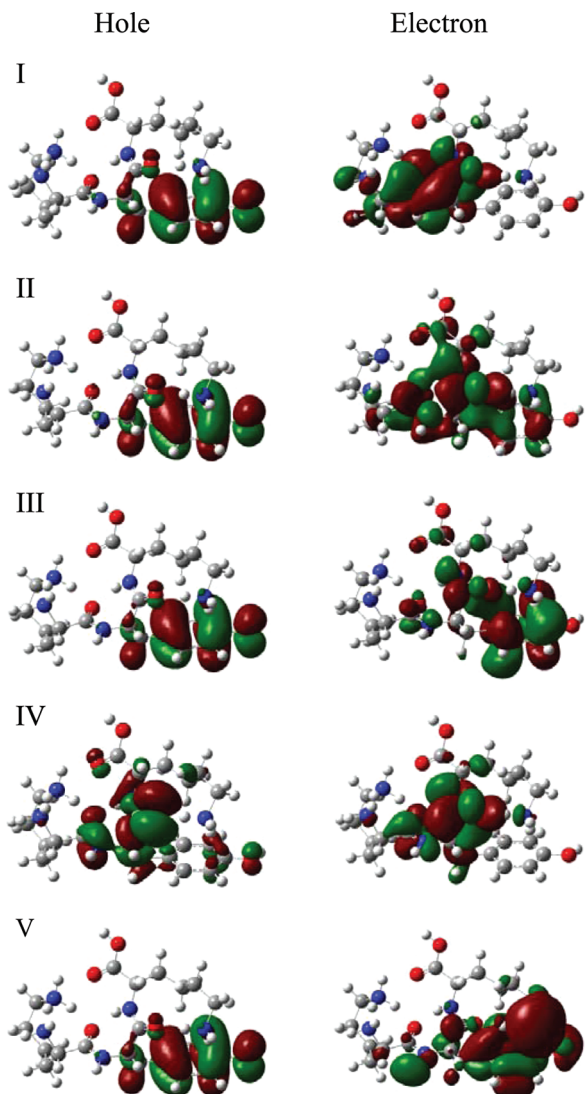


Figure 4. Dominant natural transition orbitals for the transitions with the highest oscillator strengths (I–V in Figure 3). See text for more details.

shows the time spectra for each of the ions after 270 nm photoexcitation. For the tripeptide ions, it is evident that while they all absorb at 270 nm (Figure 6d–g), absorption is lower than after 215 nm photoexcitation (Figure 5d–g). Previous work on protonated dipeptides by the Aarhus group revealed a potential limitation in measuring the absorption in the region of 270 nm using the present experimental methods.²¹ Let us consider these issues to determine whether they affect the current studies:

In delayed dissociation experiments on protonated alanine-tyrosine (AY) and tyrosine-alanine (YA) dipeptides, an absence of the 275 nm absorption band was explained as arising from a number of factors.²¹ One explanation is that the ions are decaying too fast for measurement in ELISA. This is possible after internal conversion of the photoexcited ions to a hot electronic ground state. Indeed, the dissociation lifetime of photoexcited $[YA + H]^+$ cations was found by Aravind et al.³⁵ to be 105 ± 10 ns, which is much less than the time it takes to travel from one side of the ring to the other ($23 \mu s$). A second possible mechanism limiting the measurement of absorption is hydrogen loss, which occurs due to a coupling between the

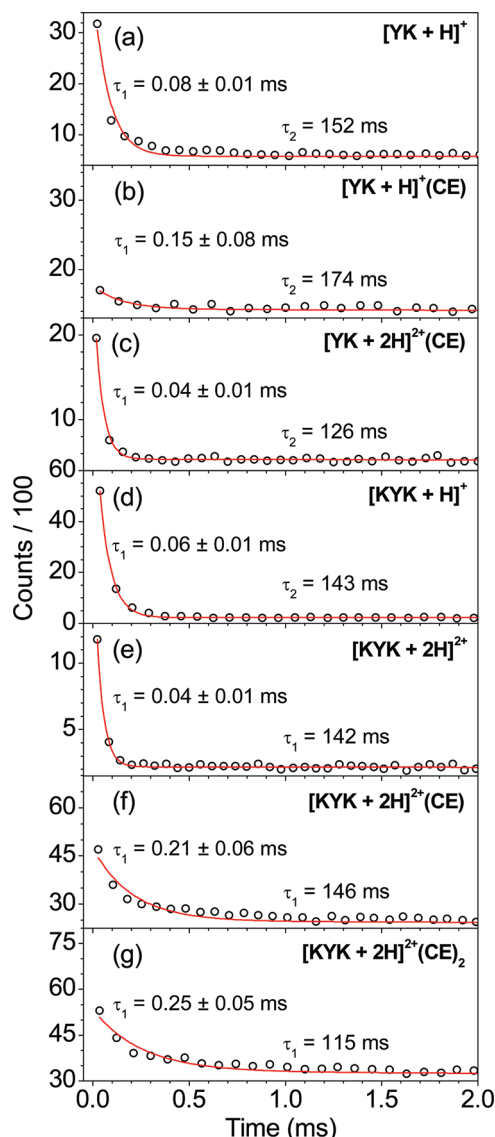


Figure 5. Time spectra of the dipeptides $[YK + H]^+$, $[YK + H]^+(CE)$, and $[YK + 2H]^{2+}(CE)$ and the tripeptides $[KYK + H]^+$, $[KYK + 2H]^{2+}$, $[KYK + 2H]^{2+}(CE)$, and $[KYK + 2H]^{2+}(CE)_2$ after 215 nm photoexcitation. The solid curves are fits of two exponentials to the data. The decay times for the photoexcited ions (<1 ms), and the ions in the ring (>100 ms) are indicated. Each spectrum is the sum of results from 2000 injections.

Table 1. Revolution Times in the ELISA Storage Ring for Each of the Studied Ions

ion	revolution time (μs)
$[YK + H]^+$	71
$[YK + H]^+(CE)$	96
$[YK + 2H]^{2+}(CE)$	68
$[KYK + H]^+$	84
$[KYK + 2H]^{2+}$	60
$[KYK + 2H]^{2+}(CE)$	76
$[KYK + 2H]^{2+}(CE)_2$	89

$\pi\pi^*(\text{phenol})$ and $\pi\sigma^*(\text{NH}_3)$ states subsequent to UV excitation of the phenol aromatic ring to a $\pi\pi^*$ state. Detection of this low mass fragment is not possible due to its low kinetic energy, and while dehydrogenated ions will continue to be

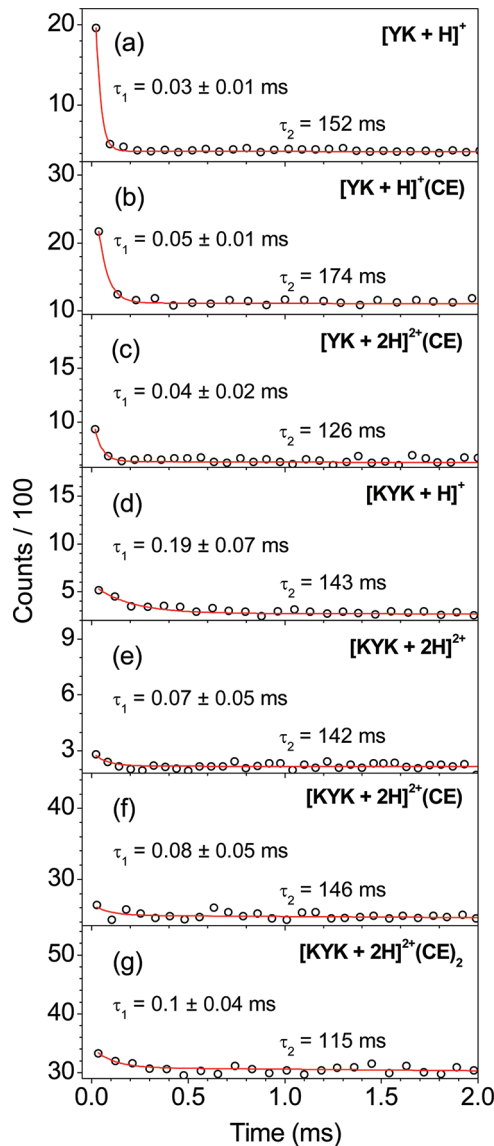


Figure 6. Time spectra of the dipeptides $[YK + H]^+$, $[YK + H]^+(CE)$, and $[YK + 2H]^{2+}(CE)$ and the tripeptides $[KYK + H]^+$, $[KYK + 2H]^{2+}$, $[KYK + 2H]^{2+}(CE)$, and $[KYK + 2H]^{2+}(CE)_2$ after 270 nm photoexcitation. The solid curves are fits of two exponentials to the data. The decay times for the photoexcited ions (<1 ms), and the ions in the ring (>100 ms) are indicated. Each spectrum is the sum of results from 2000 injections.

stored in the ring due to poor mass resolution, they will have too low an internal energy for further fragmentation within the time scale of the experiment when 270 nm photons are used. For the $[AY + H]^+$ and $[YA + H]^+$ cations, our experiment is, therefore, essentially blind to the dehydrogenation mechanism at this wavelength. Reintroduction of this missing absorption band was accomplished through complexation of the ions with CE, a molecule which targets the N-terminal ammonium group. Such complexation raises the $\pi\sigma^*$ state up in energy and likely out of the spectral region at the studied wavelengths, hence blocking the H-loss pathway. In addition, as the complex has more degrees of freedom, it has a longer lifetime with respect to statistical dissociation. A further consequence of such a complexation is that the mobile proton model that accounts for the facile breakage of peptide bonds^{36,37} is no longer operative, which implies that the activation energy for

dissociation is higher for the complex than for the bare ion itself.²¹

In order to determine whether dissociation after hydrogen loss can be sampled for tripeptides in the present work, let us consider the energies per degree of freedom in the molecules after photoabsorption. Singly protonated AY molecules gain 0.046 eV of energy per degree of freedom after absorption of 270 nm light (35 atoms; 99 degrees of freedom), with this number being reduced after hydrogen loss by an amount that relates to the binding energy. However, singly protonated KYK molecules only gain 0.030 eV of energy per degree of freedom after 210 nm photon absorption (67 atoms; 195 degrees of freedom). As this number is less than that for AY molecules after 270 nm photon absorption, it is very likely that 210 nm photoexcited KYK ions, which lose hydrogen, would also not have enough energy left to decay on the time scale of the experiment. However, work by Grégoire et al.²² showed no evidence for a photoinduced H-atom loss reaction in the case of protonated GWG and GYG (where G is glycine). Furthermore, previous work has shown that after electron capture, hydrogen loss is less likely for tripeptides than dipeptides due to the folding of the larger peptide (caging effect).³⁸ While it is likely that this is also the case after photon absorption, if hydrogen loss is occurring, our experiment is blind to it.

Statistical dissociation after internal conversion is another possible dissociation channel. As mentioned before, photo-excited dipeptide cations dissociate with a lifetime of ~ 100 ns,³⁵ which is too fast to be measured at ELISA. However, as shown in Figures 5 and 6, absorption of 215 nm and 270 nm light is seen. It can hence be concluded that for the tripeptides, the higher number of degrees of freedom increases the time scale for dissociation to time scales measurable at ELISA. Taken together, our experiment is monitoring intact tripeptide ions, which have undergone internal conversion after photoexcitation and subsequently dissociate statistically on a microsecond time scale.

For the dipeptides, the situation is not as clear. Singly protonated YK molecules gain 0.045 eV of energy per degree of freedom after absorption of 210 nm light and 0.035 eV of energy per degree of freedom after absorption of 270 nm light (46 atoms; 132 degrees of freedom). Both of these energies are less than that gained by protonated AY molecules after 270 nm light absorption (0.046 eV). Therefore, it is likely that YK ions, which lose hydrogen, would also not have enough energy left to decay on the time scale of the experiment. However, while absorption of 270 nm light is not observed for the protonated AY molecules, both 210 nm and 270 nm light absorption by the protonated YK molecules is measurable. Additionally, peptide folding has been shown to decrease the propensity for hydrogen loss after electron capture,³⁸ and the number of folding configurations of the protonated YK molecules is increased with respect to those of the protonated AY molecules due to the presence of the lysine side chain. Hydrogen loss after photon absorption is, therefore, likely to be prevented in certain configurations, leading to a measurable signal.

In Figure 5, fits to the time spectra are shown, and they comprise of two exponential components, the time constants of which are indicated in each subplot. The fast decay components are the decay rates of the ions that were excited through the absorption of a photon. Such photoexcited ions internally convert to a vibrationally hot electronic ground state from which dissociation occurs (vide supra). The longer time constant, due to collision-induced dissociation, was determined

for each species by fitting the decay of ions when no photoexcitation occurred. Note, as the first detection of neutrals is from dissociations that occurred approximately half a revolution after photoexcitation, prompt dissociations on a nanosecond time scale are not accounted for. Nonetheless, the measured dissociation rate constants provide useful information.

If we first consider the tripeptide group, it can be seen that the addition of a proton leads to a faster decay rate (decay time of 0.04 ± 0.01 ms for $[\text{KYK} + 2\text{H}]^{2+}$ in comparison with a decay time of 0.06 ± 0.01 ms for $[\text{KYK} + \text{H}]^+$, Figure 5e,d, respectively). Such an increased decay rate could be due to a number of factors including but not necessarily limited to the following: (i) loss of ammonia, which is a low-energy channel, is likely to be more prominent for the doubly protonated molecule than for the singly protonated molecule as such a dissociation can occur from either of the two charged ammoniums. (ii) Cleavage of the peptide bond. It is generally accepted that after vibrational heating of a peptide cation, the ionizing proton is no longer sequestered at the most basic site but is instead mobile and can explore less basic sites such as the amide group. Amide protonation weakens the C(O)–N bond and accounts for the formation of *y* and *b* fragments. The probability of this reaction channel occurring is likely to be increased by the presence of an additional proton as either could be involved in such cleavage. (iii) It is possible that the additional Coulomb repulsion in the doubly protonated ion increases the possibility of fragmentation. This is in agreement with experiments that determined the activation energy for dissociation of doubly protonated bradykinin to be 0.84 eV and the activation energy for dissociation of singly protonated bradykinin to be 1.3 eV.³⁹

Complexation of the tripeptide with CE leads to a longer decay time (0.21 ± 0.06 ms, Figure 5f) in accordance with the fact that the larger molecule has more degrees of freedom. Furthermore as mentioned above, such complexation reduces proton mobility and raises the activation energy for dissociation. In agreement with this explanation, it can be seen that the addition of another CE increases the decay rate further (0.25 ± 0.05 ms, Figure 5g).

As discussed above, it is possible that hydrogen loss from the bare dipeptides is skewing our results as was the case for protonated AY and YA. Even so, an equivalent pattern of lifetime increases/decreases is seen for the dipeptides with the decay rates changing from 0.08 ± 0.01 ms to 0.15 ± 0.08 ms to 0.04 ± 0.01 ms as CE and another charge are added to the protonated dipeptide (Figure 5a–c).

Absorption in the 270 nm region is in general reduced in comparison to that at 215 nm, and the fitting of the data is hence problematic (Figure 6). Nonetheless, the lifetime values change as expected. Specifically, it can be seen that for $[\text{KYK} + \text{H}]^+$ (Figure 6d), there is a decay time of 0.19 ± 0.07 ms, which decreases to 0.07 ± 0.05 ms after additional protonation (figure 6e) and increases to 0.08 ± 0.05 ms and 0.1 ± 0.04 ms after subsequent addition of either one or two crown ethers, respectively (Figure 6f,g). Similarly, for $[\text{YK} + \text{H}]^+$, the decay time changes from 0.03 ± 0.01 ms to 0.05 ± 0.01 ms after a crown ether is added and then to 0.04 ± 0.02 ms upon further protonation (Figure 6a–c).

3.3. Action Spectra. The yield of photoneutrals at each wavelength was calculated by summing the photoinduced signal in each time spectrum and correcting for ion beam fluctuations and the number of photons. The resultant action spectra are

shown in Figures 7–10. As the first data points in the time spectra are recorded after half a revolution in the ring, this

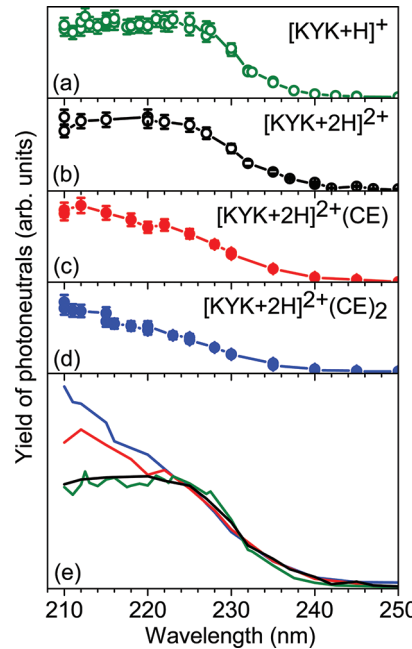


Figure 7. Action spectra from 210 to 250 nm of the tripeptides $[\text{KYK} + \text{H}]^+$, $[\text{KYK} + 2\text{H}]^{2+}$, $[\text{KYK} + 2\text{H}]^{2+}(\text{CE})$, and $[\text{KYK} + 2\text{H}]^{2+}(\text{CE})_2$. In (e), all four spectra, scaled with respect to one another, are shown.

method can introduce a negative bias toward the blue for ions that decay on faster time scales (vide infra). To circumvent this, the data can be fitted with exponentials and a number proportional to the total number of photoexcited ions calculated.⁴⁰ For the current data, the summation method was used due to the complexity of fitting data with limited points representing the decay of photoexcited ions. However, both methods produced similar spectra.

As two separate absorption bands are within the experimental range, the data for each are shown in different graphs for clarity. In the wavelength region from 210 to 250 nm (Figures 7 and 9), it can be seen that there are differences between the absorption profiles of the different ions. However, in the region from 250 to 310 nm (Figures 8 and 10), it is evident that for all ions the absorption band maxima are between 270 and 280 nm, which is in the region at which protonated tyrosine²⁵ and the complexes of protonated dipeptides AY and YA with CE also absorb.²¹ The overall trends are also rather similar to those from the calculations shown in Figure 3. However, a direct comparison with the theoretical calculations is difficult as not all of the possible structures were considered in the calculations.

Scrutiny of Figure 7e reveals that the absorption of the ions follows two trends: absorption by the ions $[\text{KYK} + \text{H}]^+$ and $[\text{KYK} + 2\text{H}]^{2+}$ is similar with a broad absorption band observed (absorption from below 210 nm to above 230 nm). Likewise, the ions $[\text{KYK} + 2\text{H}]^{2+}(\text{CE})$ and $[\text{KYK} + 2\text{H}]^{2+}(\text{CE})_2$ absorb in a comparable manner to one another with a broad absorption band seen (absorption from below 210 nm to above 230 nm). Differences between these two sets of spectra, however, are present. For the uncomplexed molecules, absorption in the 210 nm to 220 nm region is suppressed relative to that at higher wavelengths. This difference may in

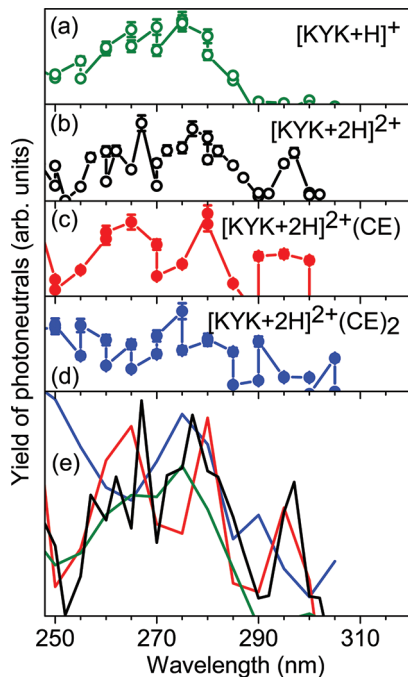


Figure 8. Action spectra from 250 to 305 nm of the tripeptides $[KYK + H]^+$, $[KYK + 2H]^{2+}$, $[KYK + 2H]^{2+}(CE)$, and $[KYK + 2H]^{2+}(CE)_2$. In (e), all four spectra, scaled with respect to one another, are shown.

part be due to the shorter lifetimes of the uncomplexed photoexcited ions in this region (Figure 5). As the first data points in the time spectra are recorded after half a revolution in the ring, this method can underestimate the absorption for ions that decay on fast time scales and introduce a negative bias for absorption to the blue due to the correlation between decay rates and excitation energy. The differences observed here, however, may not be completely attributable to such a negative bias as the spectra are similar to those calculated after fitting exponential decays to the data. It should be noted that the spectral change is caused by one crown ether and that very little happens upon addition of the second.

In Figure 9, the action spectra of the dipeptide ions in the region 210 to 250 nm are shown. As discussed above, loss of hydrogen is a possible decay channel for the dipeptides and as the branching ratios for the different decay channels may be wavelength dependent, our action spectra for the dipeptides may not be equivalent to absorption spectra. Nonetheless, in Figure 9, it can be seen that absorption in the 210 to 225 nm region is increased for this ion compared to the protonated tripeptide, a disparity that is possibly due to the different lifetimes of the photoexcited ions (0.08 ± 0.01 ms for $[KYK + H]^+$; 0.06 ± 0.01 ms for $[KYK + H]^{2+}$). Addition of a CE to the protonated dipeptide does not change the absorption dramatically. However, significant differences are seen after the addition of a second proton. There, the lifetime of the photoexcited ions is reduced to 0.04 ± 0.01 ms, and the absorption to the blue is suppressed.

For the lower energy absorption band (Figures 8 and 10), differences between the different ions are not observed. Indeed, for all of the ions, the absorption band maxima are between 270 and 280 nm. However, caution should be taken before concluding that the proximity of a charge has no effect on this absorption band as it is possible our data are not good enough to reveal any differences in the absorption in this

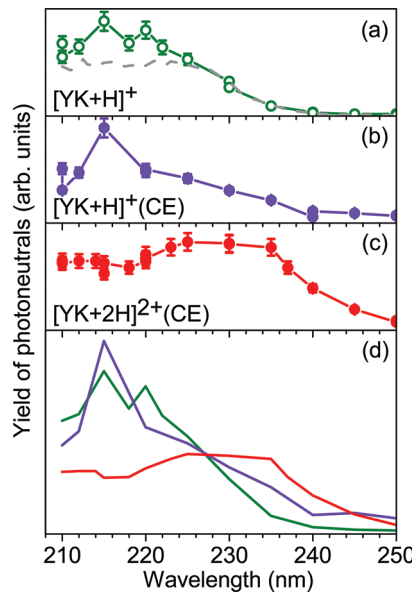


Figure 9. Action spectra from 210 to 250 nm of the dipeptides $[YK + H]^+$, $[YK + H]^{2+}(CE)$, and $[YK + 2H]^{2+}(CE)$. In (d), all three spectra, scaled with respect to one another, are shown. The action spectrum for $[YK + H]^+$ is shown for comparison purposes by a gray dashed line in the top subplot.

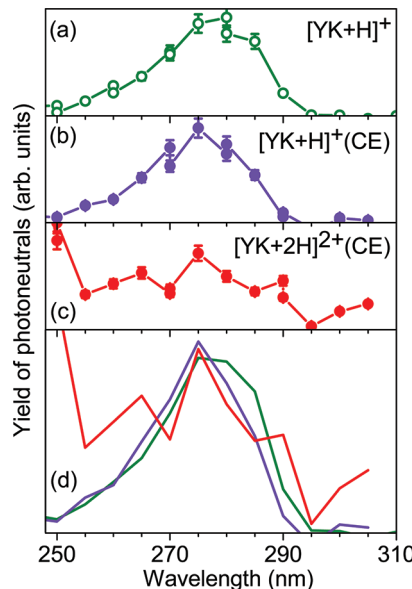


Figure 10. Action spectra from 250 to 310 nm of the dipeptides $[YK + H]^+$, $[YK + H]^{2+}(CE)$, and $[YK + 2H]^{2+}(CE)$. In (d), all three spectra, scaled with respect to one another, are shown.

region. Absorption in the 270 nm region is in general reduced in comparison to that at 215 nm (Figures 5 and 6).

4. CONCLUSIONS

Calculations predict that nearby charges should affect the absorption of $[KYK + 2H]^{2+}$. Hence, the effects of charge location and folding motifs on the absorption of tyrosine-containing peptides were studied experimentally in an electrostatic storage ring by altering the charge-chromophore interaction. Modification of this interaction was realized by varying the distance between the backbone ammonium and the chromophore, changing the charge state of the peptides, and by

altering the folding motifs using CE. Lifetimes after photoexcitation were measured and found to shorten upon protonation and lengthen upon CE complexation, in accordance with the increased number of degrees of freedom and an increase in activation energies for dissociation as the mobile proton model is no longer operative. Action spectra revealed changes in the absorption band between 210 and 250 nm, while no difference could be established with certainty for the lowest energy transition at around 275 nm. The small differences observed in the experiments suggest that a large number of isomers with slightly different absorption behaviors likely reduce the effects of a nearby charge.

AUTHOR INFORMATION

Corresponding Author

*E-mail: jeanwyer@phys.au.dk.

Notes

The authors declare no competing financial interest.

ACKNOWLEDGMENTS

S.B.N. and J.W. gratefully acknowledge support from Lundbeckfonden. C.R.C. acknowledges funding from EPSRC Postdoctoral Fellowship Scheme at the Physics-Life Science Interface. O.K. and C.R.C. also acknowledge support from Leverhulme Trust. H.Z. gratefully acknowledges support from the Swedish Research Council. Eyjafjallajokull is recognized for its contribution towards the granting of extended beam time. The experiments have been performed at the ELISA facility, an installation of the distributed LEIF Infrastructure. The support received from the ITS-LEIF Project (RII3-026015) is gratefully acknowledged.

REFERENCES

- (1) Brøndsted Nielsen, S.; Lapierre, A.; Andersen, J. U.; Pedersen, U. V.; Tomita, S.; Andersen, L. H. *Phys. Rev. Lett.* **2001**, *87*, 228102.
- (2) Andersen, L. H.; Nielsen, I. B.; Kristensen, M. B.; El Ghazaly, M. O. A.; Haacke, S.; Brøndsted Nielsen, M.; Petersen, M. Å. *J. Am. Chem. Soc.* **2005**, *127*, 12347–12350.
- (3) Nielsen, I. B.; Lammich, L.; Andersen, L. H. *Phys. Rev. Lett.* **2006**, *96*, 018304.
- (4) Lakowicz, J. R. *Principles of Fluorescence Spectroscopy*; Kluwer Academic/Plenum Publishers: New York, 1999.
- (5) Harada, I.; Takeuchi, H. In *Spectroscopy of Biological Systems*; Clark, R. J. H., Hester, R. E., Eds.; Advances in Spectroscopy 13; Wiley: New York, 1986; pp 113–175.
- (6) Kang, H.; Jouvet, C.; Dedonder-Lardeux, C.; Martrenchard, S.; Gregoire, G.; Desfrancois, C.; Schermann, J. P.; Barat, M.; Fayeton, J. A. *Phys. Chem. Chem. Phys.* **2005**, *7*, 394–398.
- (7) Lucas, B.; Barat, M.; Fayeton, J. A.; Perot, M.; Jouvet, C.; Gregoire, G.; Brøndsted Nielsen, S. *J. Chem. Phys.* **2008**, *128*, 164302.
- (8) Weinkauf, R.; Schanen, P.; Metsala, A.; Schlag, E. W.; Burgle, M.; Kessler, H. *J. Phys. Chem.* **1996**, *100*, 18567–18585.
- (9) Weinkauf, R.; Schlag, E. W.; Martinez, T. J.; Levine, R. D. *J. Phys. Chem. A* **1997**, *101*, 7702–7710.
- (10) Hu, Y. J.; Hadas, B.; Davidovitz, M.; Balta, B.; Lifshitz, C. *J. Phys. Chem. A* **2003**, *107*, 6507–6514.
- (11) Cui, W.; Hu, Y.; Lifshitz, C. *Eur. Phys. J. D* **2002**, *20*, 565–571.
- (12) Boyarkin, O. V.; Mercier, S. R.; Kamariotis, A.; Rizzo, T. R. *J. Am. Chem. Soc.* **2006**, *128*, 2816–2817.
- (13) Yoon, S. H.; Kim, M. S. *J. Am. Soc. Mass Spectrom.* **2007**, *18*, 1729–1739.
- (14) Oh, J. Y.; Moon, J. H.; Kim, M. S. *J. Mass Spectrom.* **2005**, *40*, 899–907.
- (15) Weinkauf, R.; Schanen, P.; Yang, D.; Sonkara, S.; Schlag, E. W. *J. Phys. Chem.* **1995**, *99*, 11255–11265.
- (16) Sobolewski, A. L.; Shemesh, D.; Domcke, W. *J. Phys. Chem. A* **2009**, *113*, 542–550.
- (17) Cohen, R.; Brauer, B.; Nir, E.; Grace, L.; de Vries, M. S. *J. Phys. Chem. A* **2000**, *104*, 6351–6355.
- (18) Joly, L.; Antoine, R.; Allouche, A. R.; Broyer, M.; Lemoine, J.; Dugourd, P. *J. Am. Chem. Soc.* **2007**, *129*, 8428–8429.
- (19) Joly, L.; Antoine, R.; Broyer, M.; Lemoine, J.; Dugourd, P. *J. Phys. Chem. A* **2008**, *112*, 898–903.
- (20) Andersen, L. H.; Bluhme, H.; Boye, S.; Jørgensen, T. J. D.; Krogh, H.; Nielsen, I. B.; Brøndsted Nielsen, S.; Svendsen, A. *Phys. Chem. Chem. Phys.* **2004**, *6*, 2617–2627.
- (21) Wyer, J. A.; Ehlerding, A.; Zettergren, H.; Kirketerp, M.-B. S.; Brøndsted Nielsen, S. *J. Phys. Chem. A* **2009**, *113*, 9277–9285.
- (22) Gregoire, G.; Dedonder-Lardeux, C.; Jouvet, C.; Desfrancois, C.; Fayeton, J. A. *Phys. Chem. Chem. Phys.* **2007**, *9*, 78–82.
- (23) Møller, S. P. *Nucl. Instrum. Methods Phys. Res., Sect. A* **1997**, *394*, 281–286.
- (24) Andersen, J. U.; Hvelplund, P.; Brøndsted Nielsen, S.; Tomita, S.; Wahlgreen, H.; Møller, S. P.; Pedersen, U. V.; Forster, J. S.; Jørgensen, T. J. D. *Rev. Sci. Instrum.* **2002**, *73*, 1284–1287.
- (25) Antoine, R.; Dugourd, P. *Phys. Chem. Chem. Phys.* **2011**, *13*, 16494–16509.
- (26) Bellina, B.; Compagnon, I.; Joly, L.; Albrieux, F.; Allouche, A. R.; Bertorelle, F.; Lemoine, J.; Antoine, R.; Dugourd, P. *Int. J. Mass Spectrom.* **2010**, *297*, 36–40.
- (27) Prell, J. S.; O'Brien, J. T.; Holm, A. I. S.; Leib, R. D.; Donald, W. A.; Willialms, E. R. *J. Am. Chem. Soc.* **2008**, *130*, 12680–12689.
- (28) Raevsky, O. A.; Solovev, V. P.; Solotnov, A. F.; Schneider, H. J.; Rudiger, V. *J. Org. Chem.* **1996**, *61*, 8113–8116.
- (29) Julian, R. R.; Beauchamp, J. L. *Int. J. Mass Spectrom.* **2001**, *210*, 613–623.
- (30) Wilson, J. J.; Kirkovits, G. J.; Sessler, J. L.; Brodbelt, J. S. *J. Am. Soc. Mass Spectrom.* **2008**, *19*, 257–260.
- (31) Andersen, J. U.; Cederquist, H.; Forster, J. S.; Huber, B. A.; Hvelplund, P.; Jensen, J.; Liu, B.; Manil, B.; Maunoury, L.; Brøndsted Nielsen, S.; Pedersen, U. V.; Rangama, J.; Schmidt, H. T.; Tomita, S.; Zettergren, H. *Phys. Chem. Chem. Phys.* **2004**, *6*, 2676–2681.
- (32) Frisch, M. J.; Trucks, G. W.; Schlegel, H. B.; Scuseria, G. E.; Robb, M. A.; Cheeseman, J. R.; Montgomery, J. A., Jr.; Vreven, T.; Kudin, K. N.; Burant, J. C.; Millam, J. M.; Iyengar, S. S.; Tomasi, J.; Barone, V.; Mennucci, B.; Cossi, M.; Scalmani, G.; Rega, N.; Petersson, G. A.; Nakatsuji, H.; Hada, M.; Ehara, M.; Toyota, K.; Fukuda, R.; Hasegawa, J.; Ishida, M.; Nakajima, T.; Honda, Y.; Kitao, O.; Nakai, H.; Klene, M.; Li, X.; Knox, J. E.; Hratchian, H. P.; Cross, J. B.; Bakken, V.; Adamo, C.; Jaramillo, J.; Gomperts, R.; Stratmann, R. E.; Yazev, O.; Austin, A. J.; Cammi, R.; Pomelli, C.; Ochterski, J. W.; Ayala, P. Y.; Morokuma, K.; Voth, G. A.; Salvador, P.; Dannenberg, J. J.; Zakrzewski, V. G.; Dapprich, S.; Daniels, A. D.; Strain, M. C.; Farkas, O.; Malick, D. K.; Rabuck, A. D.; Raghavachari, K.; Foresman, J. B.; Ortiz, J. V.; Cui, Q.; Baboul, A. G.; Clifford, S.; Cioslowski, J.; Stefanov, B. B.; Liu, G.; Liashenko, A.; Piskorz, P.; Komaromi, I.; Martin, R. L.; Fox, D. J.; Keith, T.; Al-Laham, M. A.; Peng, C. Y.; Nanayakkara, A.; Challacombe, M.; Gill, P. M. W.; Johnson, B.; Chen, W.; Wong, M. W.; Gonzalez, C.; Pople, J. A. *Gaussian 03*, revision D.01; Gaussian, Inc.: Wallingford, CT, 2003.
- (33) Martin, R. L. *J. Chem. Phys.* **2003**, *118*, 4775–4777.
- (34) Kirketerp, M. B. S.; Ryhding, T.; Støckkel, K.; Nielsen, M. B.; Brøndsted Nielsen, S. *J. Phys. Chem. A* **2011**, *115*, 1222–1227.
- (35) Aravind, G.; Klarke, B.; Rajput, J.; Toker, Y.; Andersen, L. H.; Bochenkova, A. V.; Antoine, R.; Lemoine, J.; Racaud, A.; Dugourd, P. *J. Chem. Phys.* **2012**, *136*, 014307.
- (36) Wysocki, V. H.; Resing, K. A.; Zhang, Q. F.; Cheng, G. L. *Methods* **2005**, *35*, 211–222.
- (37) Wysocki, V. H.; Tsaprailis, G.; Smith, L. L.; Breci, L. A. *J. Mass Spectrom.* **2000**, *35*, 1399–1406.
- (38) Chakraborty, T.; Holm, A. I. S.; Hvelplund, P.; Brøndsted Nielsen, S.; Pouilly, J. C.; Worm, E. S.; Williams, E. R. *J. Am. Soc. Mass Spectrom.* **2006**, *17*, 1675–1680.

- (39) Schnier, P. D.; Price, W. D.; Jockusch, R. A.; Williams, E. R. *J. Am. Chem. Soc.* **1996**, *118*, 7178–7189.
(40) Wyer, J. A.; Brøndsted Nielsen, S. *J. Chem. Phys.* **2010**, *133*, 084306.